

Highly selective C=C bond hydrogenation in α,β -unsaturated ketones catalyzed by hectorite-supported ruthenium nanoparticles

Farooq-Ahmad Khan^a, Armelle Vallat^b, Georg Süß-Fink^{a,*}

^a Institut de Chimie, Université de Neuchâtel, CH-2000 Neuchâtel, Switzerland

^b Service Analytique Facultaire, Université de Neuchâtel, CH-2000 Neuchâtel, Switzerland

ABSTRACT

Metallic ruthenium nanoparticles intercalated in hectorite (particle size ~ 7 nm) were found to catalyze the specific hydrogenation (conversion 100%, selectivity $> 99.9\%$) of the carbon-carbon double bond in α,β -unsaturated ketones such as 3-buten-2-one, 3-penten-2-one, 4-methyl-3-penten-2-one. The catalytic turnovers range from 765 to 91,800, the reaction conditions being very mild (temperature 35°C and constant hydrogen pressure 1–10 bar). After a catalytic run, the catalyst can be recycled and reused without loss of activity and selectivity

Keywords

Ruthenium nanoparticles, Ruthenium-modified hectorite, Selective C=C bond hydrogenation, Selective hydrogenation of unsaturated ketones, Mesityl oxide reduction

1. Introduction

Chemoselective hydrogenation of α,β -unsaturated carbonyl compounds is useful in the preparation of fine chemicals, flavors, hardening of fats, pharmaceutical manufacturing processes and in the synthesis of various organic intermediates and solvents [1]. The selectivity of the reaction is a problem and requires specific reaction conditions and catalyst systems. In heterogeneous catalysts, the effect of metal-support interaction also plays an important role in determining the selectivity of the reaction [2]. Therefore, the design of nanocomposites consisting of functional metals and adequate matrices is a challenge for the fabrication of recyclable catalysts. Highly active metallic nanoparticles must be stabilized by a suitable support in order to prevent aggregation to bulk metal [3]. Hectorite is a naturally occurring clay, belonging to the smectite family of layered minerals. These materials are composed of individual platelets containing a metal oxide center sandwiched between two silicone dioxide outer layers. Included in this group of minerals are sodium hectorite, bentonite (montmorillonite), saponite, vermiculite, kenyaite, volkonskoite, sepiolite, beidellite, magadiite, nontronite and saucanite. Of these,

hectorite is the most important one because of its exceptional swelling properties. It can be defined as layers of negatively charged two-dimensional silicate sheets held together by cationic species in the interlaminar space, which are susceptible to ion exchange [4–6]. Ruthenium-supported hectorite obtained by ion exchange has been reported by Shimazu et al. using $[\text{Ru}(\text{NH}_3)_6]^{2+}$ cations [7] and by our group using $[(\text{C}_6\text{H}_6)\text{Ru}(\text{H}_2\text{O})_3]^{2+}$ cations [8] or $[(\text{C}_6\text{H}_6)_4\text{Ru}_4\text{H}_4]^{2+}$ cations [9] for the intercalation. These materials show high catalytic activity for the hydrogenation of olefins [7] and of aromatic compounds [10,11]. Recently, we reported the highly selective low-temperature hydrogenation of furfuryl alcohol to tetrahydrofurfuryl alcohol catalyzed by hectorite-supported nanoparticles [12].

The hydrogenation of α,β -unsaturated ketones implies either the olefinic C=C bond or the carbonyl C=O bond, or both of them. In addition, side reactions have to be considered as well [2]. Supported metals such as platinum, rhodium, ruthenium, gold, nickel, aluminum, copper and iron are reported to be active for the hydrogenation of α,β -unsaturated ketones [13]. However, in most cases the selectivity for C=C bond hydrogenation is only high at low conversion [14,16]. Therefore, palladium is conventionally used to selectively reduce C=C bond in unsaturated carbonyl compounds [15,16]. Complex metal hydrides such as potassium triphenylborohydride and lithium aluminum hydride-copper(I) iodide also show a good selectivity (upto 99%) for olefinic bond hydrogenation in both cyclic and acyclic enones, but they result in the production of substantial amounts of waste [17]. Some organometallic complexes

* Corresponding author at: Institut de Chimie, Université de Neuchâtel, Avenue de Bellevaux 51, CH-2000 Neuchâtel, Switzerland. Tel.: +41 32 7182400; fax: +41 32 7182511.

E-mail address: georg.suess-fink@unine.ch (G. Süß-Fink).

are also highly selective toward the hydrogenation of C=C bond in α,β -unsaturated ketones under milder conditions [18]. These complexes are sensitive to permanent deactivation and show all disadvantages of homogeneous catalysts. Metal-free approaches toward such hydrogenations are almost futile with a 75% selectivity toward saturated ketones [19].

We have been interested in the influence of increasing steric hindrance at the C=C bond of α,β -unsaturated ketones on the selectivity of the hydrogenation using our hectorite-supported nano-ruthenium [8–12] as catalyst. Therefore, 3-buten-2-one, 3-penten-2-one and 4-methyl-3-penten-2-one have been studied. Of these three substrates, 4-methyl-3-penten-2-one is the most important industrial precursor; it is also called mesityl oxide which, upon selective hydrogenation, gives methyl isobutyl ketone. Methyl isobutyl ketone is an important commercial solvent with a reported world consumption of 295 thousand metric tons in 2007 [20].

Traditionally, methyl isobutyl ketone is manufactured via a three-step process in which acetone condensation gives diacetone alcohol which readily dehydrates into mesityl oxide. The olefinic C=C bond in mesityl oxide is then selectively hydrogenated to methyl isobutyl ketone avoiding further C=O reduction into methyl isobutyl carbinol. Methyl isobutyl ketone production may also be achieved by using a bifunctional catalyst to facilitate all three reaction steps in single step. A 20–60% conversion of acetone with 30–90% selectivity for methyl isobutyl ketone is observed for these single-step processes under harsh reaction conditions (80–160 °C, 10–100 bar H₂) [1b,21]. Thus, the methyl isobutyl ketone concentration in the effluent is typically less than 30 wt.% necessitating further purification steps [1b]. The large-scale production of methyl isobutyl ketone still follows the three-step route [22] involving mesityl oxide hydrogenation into methyl isobutyl ketone at 150–200 °C and 3–10 bar H₂ using Cu or Ni catalysts [23] or, alternatively, on a supported palladium catalyst at 80–220 °C [15d–f]. It is therefore desirable to find alternative green processes, which produce methyl isobutyl ketone under mild reaction conditions. Metallic ruthenium nanoparticles intercalated in hectorite are promising as catalysts, since they can be easily handled and recycled.

In this paper, we report ruthenium nanoparticles (~7 nm) intercalated in hectorite to be a highly productive (conversion 100%, turnover number 765–91,800) and highly selective (selectivity >99.9%) reusable catalyst for the hydrogenation of various industrially important α,β -unsaturated ketones under mild conditions (ethanol solution, 35 °C, 1–10 bar H₂). To the best of our knowledge, such a high selectivity with a complete conversion of mesityl oxide into methyl isobutyl ketone at mild conditions has never been reported in published literature, except for a sodium hydride containing complex reducing agent, but giving only a turnover number of 20 [17e].

2. Experimental

2.1. Syntheses

White sodium hectorite (**1**) was prepared according to the method of Bergk and Woldt [24]. The sodium cation exchange capacity, determined according to the method of Lagaly and Tributh [25], was found to be 104 meq per 100 g. The dimeric complex [(C₆H₆)₂RuCl₂]₂ was synthesized following the procedure reported by Arthur and Stephenson [26].

2.1.1. Preparation of the ruthenium(II)-containing hectorite **2**

The neutral complex [(C₆H₆)₂RuCl₂]₂ (83.8 mg, 0.17 mmol) was dissolved in distilled and Ar-saturated water (50 mL), giving a

clear yellow solution after intensive stirring for 1 h. The pH of this solution was adjusted to 8 (using a glass electrode) by adding the appropriate amount of 0.1 M NaOH. After filtration this solution was added to 1 g of finely powdered and degassed (1 h high vacuum, then Ar-saturated) sodium hectorite **1**. The resulting suspension was stirred for 4 h at 20 °C. Then the yellow ruthenium(II)-containing hectorite **2** was filtered off and dried *in vacuo*.

2.1.2. Preparation of the ruthenium(0)-containing hectorite **3** by reduction with molecular hydrogen

The ruthenium(0)-containing hectorite **3** was obtained by reacting a suspension of the yellow ruthenium(II)-containing hectorite **2** (50 mg, 0.01592 mmol Ru) in a magnetically stirred stainless-steel autoclave (volume 100 mL) under a pressure of H₂ (50 bar) at 100 °C for 14 h using ethanol (5 mL) as solvent. After pressure release and cooling for 48 h, **3** was isolated as a black material.

2.2. Catalysis

The hydrogenation of α,β -unsaturated ketones was carried out in a magnetically stirred stainless-steel autoclave. The air in the autoclave was displaced by purging three times with hydrogen prior to use. Quantitative chemical analysis of hydrogenation products was done by GC–MS analysis. The GC separation was carried out on a ZB-5MS column (30 m × 0.25 mm, 0.25 μ m) using a temperature program of 35–200 °C at 5 °C/min. The instrument used was a ThermoFinnigan® Trace GC-Polaris Q. The data were collected by using extracted ion chromatograms of marker *m/z* values for each molecule from the total ion chromatograms (TIC).

A freshly prepared suspension (5 mL) of ruthenium(0)-containing hectorite **3** was used, ethanol (15 mL) as well as corresponding α,β -unsaturated ketone (12.2 mmol) was added. Then the autoclave was heated at 35 °C under constant hydrogen pressure (1–10 bar). After 1 h, the pressure was released, the solution was filtered (0.22 μ m, PTFE) and analyzed by GC–MS in order to determine the substrate conversion and selectivity (in %). The turnover number for 3-buten-2-one and 3-penten-2-one was determined by adding 12.2 mmol of substrate in regular intervals, until the catalyst lost its selectivity. However, in the case of 4-methyl-3-penten-2-one, 122 mmol of substrate was added in regular intervals, until the catalyst lost its activity.

3. Results and discussion

Synthetic sodium hectorite (**1**) is a white solid which presents an idealized cell formula of Mg_{5.5}Li_{0.5}Si₈O₂₀(OH)₄Na·*n*H₂O. It has a three-layer sheet-like morphology which results from the two-dimensional condensation of silicic acid, two layers of SiO₄ tetrahedra being connected by a layer of MgO₆ octahedra. Partial replacement of the Mg²⁺ cations in the octahedral layers by Li⁺ cations leads to an excess of anionic charges of the layers, which are compensated by Na⁺ cations in the interlaminal space (Fig. 1). Hydratization of the interlaminal sodium cations to give [Na(H₂O)_{*n*}]⁺ is responsible for the swelling of hectorite in water, since the interlaminal space is widened [27].

Contrary to the magnesium and lithium cations in the octahedral layer, the sodium cations in the interlaminal space are not bound to the silicate framework. For this reason, the Na⁺ cations can easily be exchanged in water by other water-soluble inorganic, organic or organometallic cations. The dinuclear complex benzene ruthenium dichloride dimer dissolves in water with hydrolysis to give, with successive substitution of chloro ligands by aqua ligands, a mixture of mononuclear benzene ruthenium complexes being in equilibrium [28]. The ¹H NMR signals of the D₂O solution have been assigned to [(C₆H₆)RuCl₂(H₂O)] (δ = 5.89 ppm),

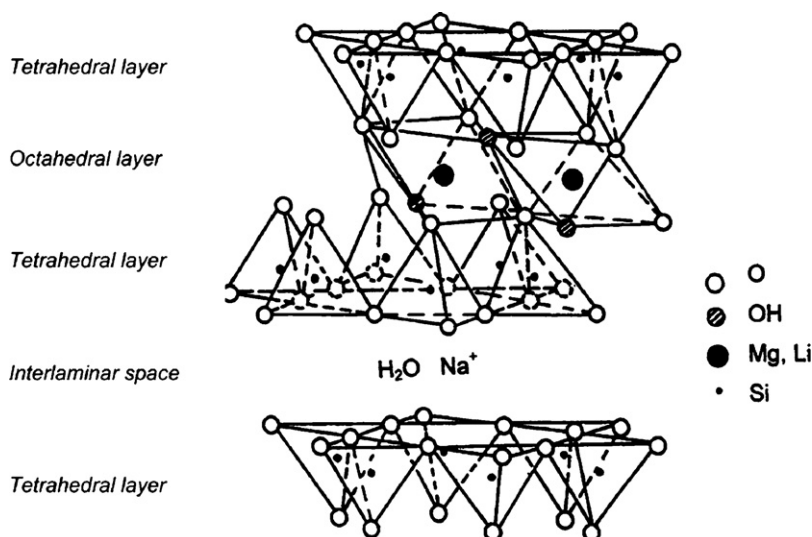


Fig. 1. Structural model according to Grim [27] of sodium hectorite $\text{Mg}_{5.5}\text{Li}_{0.5}\text{Si}_8\text{O}_{20}(\text{OH})_4\text{Na}\cdot n\text{H}_2\text{O}$, showing the anionic three-layer sheets and the interlamellar space containing sodium cations and water molecules.

$[(\text{C}_6\text{H}_6)\text{Ru}(\text{H}_2\text{O})_2]^{2+}$ ($\delta = 5.97$ ppm), and $[(\text{C}_6\text{H}_6)\text{Ru}(\text{H}_2\text{O})_3]^{2+}$ ($\delta = 6.06$ ppm) (Scheme 1) [28]. The dication $[(\text{C}_6\text{H}_6)\text{Ru}(\text{H}_2\text{O})_3]^{2+}$, which has been isolated as the sulfate and structurally characterized [29], is the major species present in the hydrolytic mixture over the pH range from 5 to 8, according to the NMR spectrum (Scheme 1).

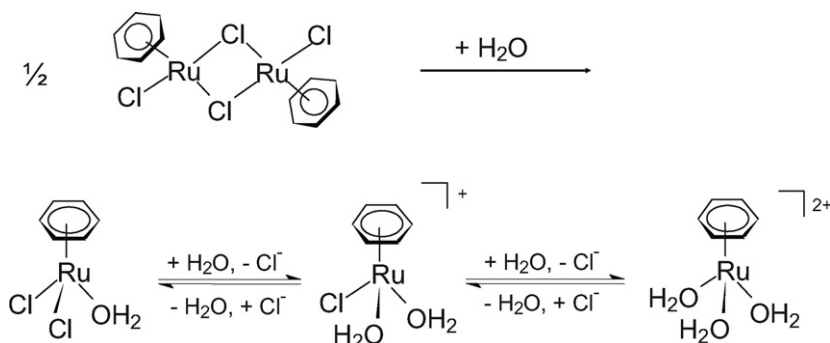
When the yellow solution obtained by dissolving the dinuclear complex $[(\text{C}_6\text{H}_6)_2\text{Ru}_2\text{Cl}_4]$ in water is added to white sodium hectorite (**1**), the main hydrolysis product $[(\text{C}_6\text{H}_6)\text{Ru}(\text{H}_2\text{O})_3]^{2+}$ intercalates into the solid, replacing the appropriate amount of sodium cations, to give the yellow ruthenium(II)-modified hectorite **2**. This material, which can be dried and stored in air, reacts with ethanolic solution of **2** under hydrogen pressure (50 bar) at 100°C by reduction of $[(\text{C}_6\text{H}_6)\text{Ru}(\text{H}_2\text{O})_3]^{2+}$ to give the black ruthenium(0)-modified hectorite **3** (Scheme 2).

The presence of metallic ruthenium was proven by its typical X-ray reflections. The specific surface of **3** was determined to be $207\text{ m}^2/\text{g}$ by adsorption techniques [8]. The ruthenium loading was assumed to be 3.2 wt.%, based upon the molar ratio of $[(\text{C}_6\text{H}_6)\text{Ru}(\text{H}_2\text{O})_3]^{2+}$ used (corresponding to 75% of the experimentally determined [25] cation exchange capacity of **1**); the ruthenium loading determined by ICP-OES of 3.4 wt.% is found to be a little too high. The size distribution of the ruthenium(0) nanoparticles in **3** was studied by transmission electron microscopy (TEM) using the “ImageJ” software [30] for image processing and analysis. The

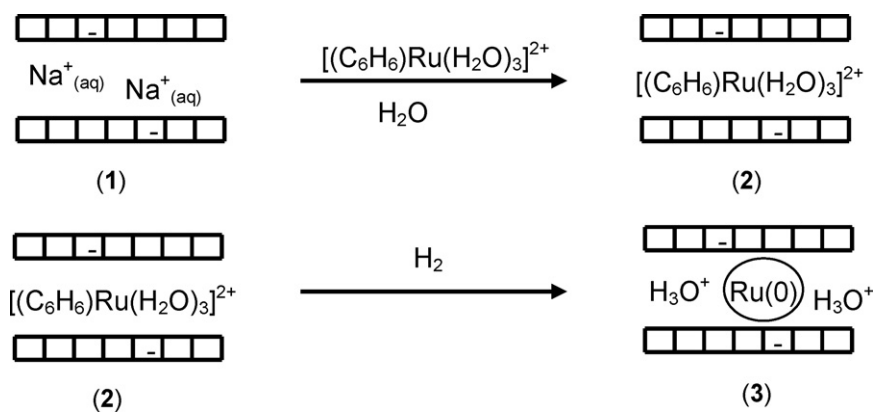
micrographs show particles of a size up to 18 nm. At the edges of superimposed silicate layers nanoparticles are visible, the lighter tone of which is typical for intercalated particles. The mean particle size and standard deviation (σ) were estimated from image analysis of *ca.* 500 particles at least. We have shown earlier that ruthenium(0) nanoparticles intercalated in hectorite can have different shapes (hexagonal or spherical) and sizes (nanoparticle size 4–38 nm), depending on the reaction conditions for the reduction step [11]. The ruthenium(0)-containing hectorite **3** prepared here has a mean particle size of 7 nm (Fig. 2).

A comparison of the diffractogram for ruthenium(0)-containing hectorite **3** with the powder pattern of sodium-containing hectorite (**1**) and ruthenium(II)-containing hectorite **2** is shown in Fig. 3. The d -spacing value ($d_{001} = 17.8\text{ \AA}$) is significantly higher for **3** than that of **1** ($d_{001} = 13.32\text{ \AA}$). The ruthenium(II)-containing hectorite **2** also shows a slight shift ($d_{001} = 14.08\text{ \AA}$) as compared to that of **1**. Peaks of the Ru phase are not observed, which is presumably due to the low concentration of Ru nanocrystallites, the peaks of which being hidden by the high hectorite background.

These ruthenium nanoparticles intercalated in hectorite are highly active and selective hydrogenation catalysts: Ruthenium(0)-containing hectorite **3** efficiently reduces different α,β -unsaturated ketones to give saturated ketones under mild conditions, the formation of the alcohols (saturated and unsaturated) being avoided. The catalytic reaction is followed by gas chromatography coupled



Scheme 1. Hydrolysis of the dinuclear complex $[(\text{C}_6\text{H}_6)_2\text{Ru}_2\text{Cl}_4]$ in water to give a mixture of mononuclear benzene ruthenium complexes, the dicationic triqua complex $[(\text{C}_6\text{H}_6)\text{Ru}(\text{H}_2\text{O})_3]^{2+}$ being the major product.



Scheme 2. Ion exchange of Na^+ cations in sodium hectorite **1** (white) against $[(\text{C}_6\text{H}_6)\text{Ru}(\text{H}_2\text{O})_3]^{2+}$ cations to give ruthenium(II)-modified hectorite **2** (yellow) and reduction of $[(\text{C}_6\text{H}_6)\text{Ru}(\text{H}_2\text{O})_3]^{2+}$ in **2** by molecular hydrogen gives ruthenium nanoparticles in the ruthenium(0)-containing hectorite **3**.

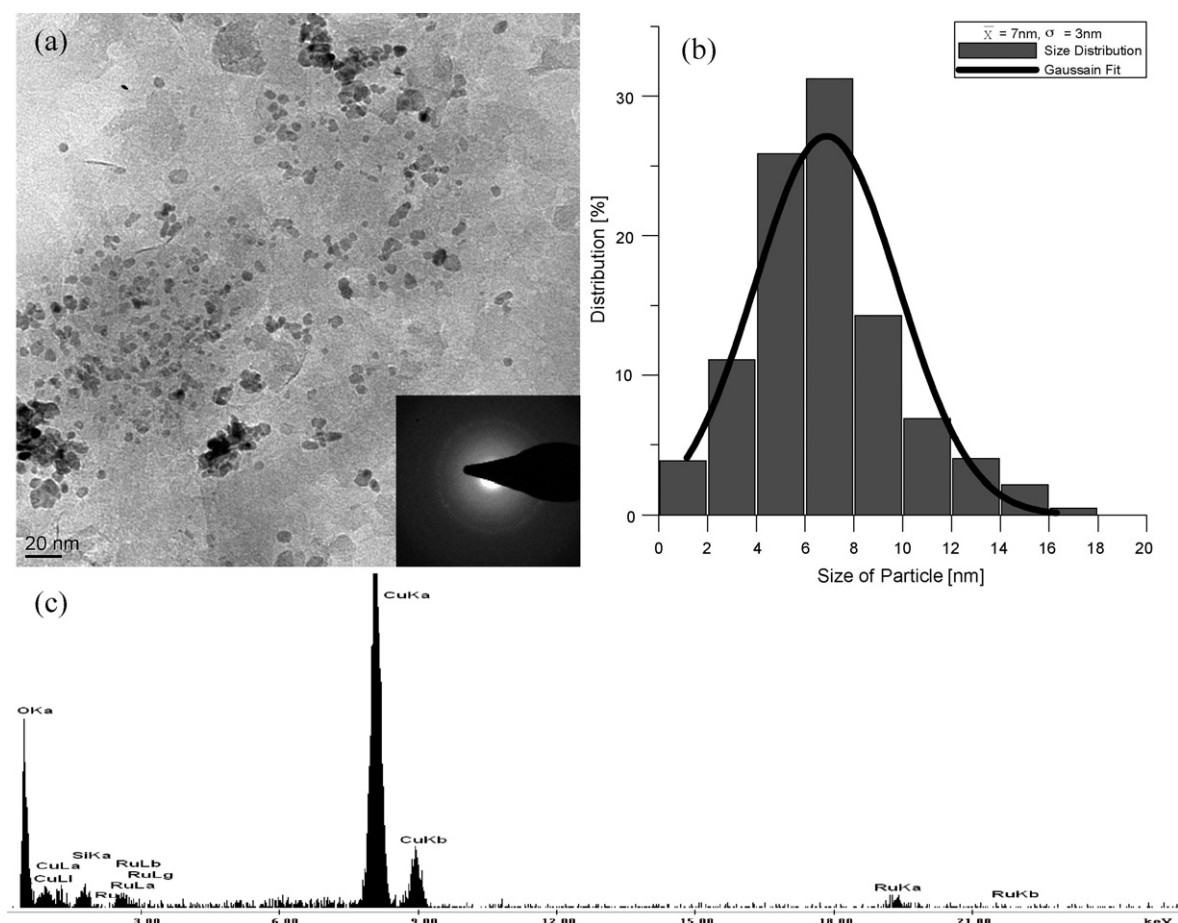
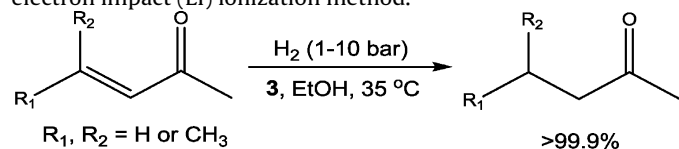


Fig. 2. TEM micrograph with SAED (a) histogram (b) and EDAX analysis (c) of ruthenium(0) nanoparticles in **3**.

to mass detector. The products are separated on an apolar column and are identified by their retention time and mass spectrum using electron impact (EI) ionization method.



For 3-buten-2-one and 3-penten-2-one hydrogenation, catalyst **3** can be used only 2 times without loss of selectivity. However, in the case of 4-methyl-3-penten-2-one hydrogenation, catalyst **3**

can be used up to 12 times until it becomes inactive. The highly productive reduction of mesityl oxide to methyl isobutyl ketone by hectorite-supported ruthenium nanoparticles is striking, especially, since no traces of further C=O reduction (methyl isobutyl carbinol) observed. This highly selective C=C bond hydrogenation is also observed for other α,β -unsaturated ketones. Low catalyst loading is capable of reducing only the olefinic double bond. The molar ratio of converted substrate to catalyst decreased in the order 4-methyl-3-penten-2-one > 3-penten-2-one > 3-buten-2-one in the direction of decreasing steric hindrance. The increasing steric hindrance in the substrate requires increased hydrogen

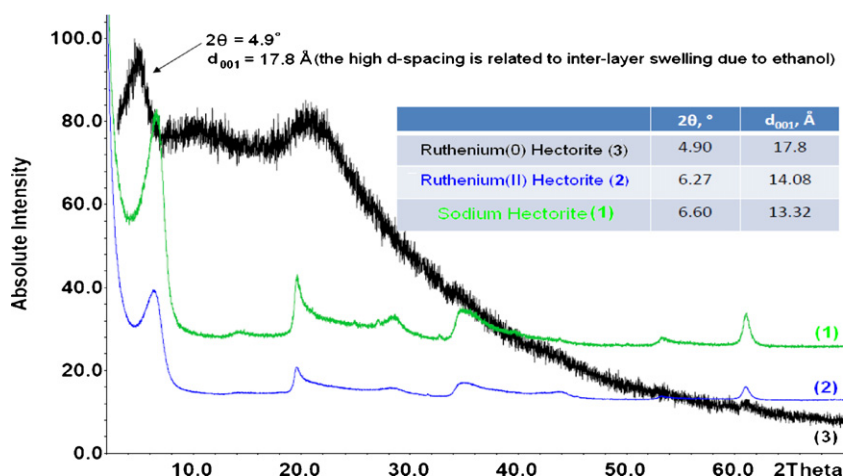


Fig. 3. XRD pattern for sodium-containing hectorite (1), ruthenium(II)-containing hectorite (2) and Ru(0)-containing hectorite (3).

Table 1

Selective hydrogenation of different α,β -unsaturated ketones by metallic ruthenium nanoparticles intercalated in hectorite.

Substrate	Pressure (bar)	Temp (°C)	Time ^a (h)	Conversion (%)	Selectivity (%)	TOF ^b (h ⁻¹)	TON ^c
3-Buten-2-one	1	35	2	100	>99.9	822	765
3-Penten-2-one	7	35	1	100	>99.9	1254	3825
4-Methyl-3-penten-2-one	10	35	1	100	>99.9	1212	91,800

^a Time required for 100% conversion of 12.2 mmol unsaturated ketones into saturated ketones.

^b Turnover frequency calculated as moles of saturated ketone per mol ruthenium per hour for 12.2 mmol substrate hydrogenation after 25 min.

^c Total turn over number (until the catalyst loses its selectivity or activity).

pressure: while 3-buten-2-one is hydrogenated under 1 bar hydrogen pressure, for 3-penten-2-one a hydrogen pressure of 7 bar is required, and for the bulkiest substrate 4-methyl-3-penten-2-one 10 bar. However, the selectivity for C=C bond hydrogenation is not reduced by the high pressure (Table 1). It is likely that the absence of bulky substituents on the conjugated C=C double bond of 3-buten-2-one favors stable adsorption of the product on catalytic sites. The high selectivity for the C=C bond hydrogenation of these α,β -unsaturated ketones can be tentatively attributed to the activation of the C=C bond by the metal-support interaction [31]. It can be assumed that hectorite probably modifies the electronic properties of ruthenium, which in turn leads to an increase in the hydrogenation selectivity for the C=C bond. Thus, the specific hydrogenation tendency of α,β -unsaturated ketones can be interpreted in terms of an exclusive adsorption of C=C bonds at the surface of these nanoparticles. The same metal-support effect was observed in the highly selective C=C bond hydrogenation of furfuryl alcohol by hectorite-supported ruthenium nanoparticles [12].

4. Conclusion

Ruthenium nanoparticles intercalated in hectorite are found to efficiently catalyze the hydrogenation of α,β -unsaturated ketones at mild conditions. The best results were obtained at 35 °C under a constant hydrogen pressure of 1–10 bar (conversion 100%, selectivity > 99.9%). Surprisingly, an exceptionally high catalytic activity is observed in the case of mesityl oxide hydrogenation. Methyl isobutyl ketone is produced in high yield with essentially all of mesityl oxide converted to methyl isobutyl ketone, and further hydrogenation of methyl isobutyl ketone does not occur. Hectorite-supported ruthenium nanoparticles can be recycled and reused.

Acknowledgments

Financial support of this work from the Fonds National Suisse de la Recherche Scientifique is gratefully acknowledged. We also

thank the Johnson Matthey Research Centre for a generous loan of ruthenium(III) chloride hydrate.

References

- (a) Y.-C. Son, S.L. Suib, R.E. Malz, in: D.G. Morrel (Ed.), *Catalysis of Organic Reactions*, Marcel Dekker Inc., New York, 2003, pp. 559–564; (b) W.K. O'Keefe, F.T.T. Ng, G.L. Rempel, *Ind. Eng. Chem. Res.* 46 (2007) 716–725; (c) P.G.N. Mertens, P. Vandezande, X. Ye, H. Poelman, I.F.J. Vankelecom, D.E. De Vos, *Appl. Catal. A: Gen.* 355 (2009) 176–183.
- P. Kluson, L. Cerveny, *Appl. Catal. A: Gen.* 128 (1995) 13–31.
- D. Astruc, F. Lu, J.R. Aranzaes, *Angew. Chem. Int. Ed.* 44 (2005) 7852–7872.
- T.J. Pinnavaia, *Science* 220 (1983) 365–371.
- J.L. Valverde, A. de Lucas, P. Sánchez, F. Dorado, A. Romero, *Appl. Catal. B* 43 (2003) 43–56.
- B.M. Choudary, M.L. Kantam, K.V.S. Ranganath, K.K. Rao, *Angew. Chem. Int. Ed.* 44 (2005) 322–325.
- S. Shimazu, T. Hirano, T. Uematsu, *Appl. Catal.* 34 (1987) 255–261.
- A. Meister, G. Meister, G. Süß-Fink, *J. Mol. Catal.* 92 (1994) L123–L126.
- A. Meister, G. Süß-Fink, Unpublished. See A. Meister, PhD Thesis, University of Neuchâtel, Switzerland, 1994.
- G. Süß-Fink, B. Mollwitz, B. Therrien, M. Dadrás, G. Laurenczy, A. Meister, G. Meister, *J. Cluster Sci.* 18 (2007) 87–95.
- G. Süß-Fink, F.-A. Khan, J. Boudon, V. Spassov, *J. Cluster Sci.* 20 (2009) 341–353.
- F.-A. Khan, A. Vallat, G. Süß-Fink, *Catal. Commun.* 12 (2011) 1428–1431.
- (a) V. Ponc, *Appl. Catal. A: Gen.* 149 (1997) 27–48; (b) J.G. de Vries, L. Lefort, P.H. Phua, *PCT Int. Appl. A1* (2009), WO 2009/150173.
- (a) E. Breitner, E. Roginski, P.N. Rylander, *J. Org. Chem.* 24 (1959) 1855–1857; (b) C. Milone, R. Ingoglia, A. Pistone, G. Neri, F. Frusteri, S. Galvagno, *J. Catal.* 222 (2004) 348–356; (c) C. Milone, R. Ingoglia, M.L. Tropeano, G. Neri, S. Galvagno, *Chem. Commun.* (2003) 868–869; (d) K.Yu. Koltunov, I.B. Repinskaya, G.I. Borodkin, *Russ. J. Org. Chem.* 37 (2001) 1534–1541.
- (a) G. Szöllösi, Á. Mastalir, Á. Molnár, M. Bartók, *React. Kinet. Catal. Lett.* 57 (1996) 29–33; (b) M.L.A. von Holleben, M. Zucolotto, C.A. Zini, E.R. Oliveira, *Tetrahedron* 50 (1994) 973–978; (c) K. Kindler, K. Lihns, *Justus Liebig's Ann. Chem.* 685 (1965) 36; (d) T. Yasuhiko, N. Toschio, *Jpn. Pat.* 61085343A, 1986.; (e) O. Norio, T. Masayuki, N. Yoshitaka, H. Shigeo, *Jpn. Pat.* 229904A, 2000.; (f) O. Norio, T. Masayuki, K. Takako, H. Shigetada, *Jpn. Pat.* 219649 A, 2000; (g) Y. Hu, H. Yang, Y. Zhang, Z. Hou, X. Wang, Y. Qiao, H. Li, B. Feng, Q. Huang, *Catal. Commun.* 10 (2009) 1903–1907; (h) A.M.R. Galletti, C. Antonetti, A.M. Venezia, G. Giambastiani, *Appl. Catal. A: Gen.* 386 (2010) 124–131.

- [16] (a) B.P.S. Chauhan, J.S. Rathore, T. Bando, *J. Am. Chem. Soc.* 126 (2004) 8493–8500;
 (b) U.R. Pillai, E. Sahle-Demessie, *J. Mol. Catal. A: Chem.* 222 (2004) 153–158;
 (c) W.K. O'Keefe, M. Jiang, F.T.T. Ng, G.L. Rempel, *Chem. Eng. Sci.* 60 (2005) 4131–4140;
 (d) Q. Liu, J. Li, X.-X. Shen, R.-G. Xing, J. Yang, Z. Liu, B. Zhou, *Tetrahedron Lett.* 50 (2009) 1026–1028.
- [17] (a) L. Mordenti, J.J. Brunet, P. Caubere, *J. Org. Chem.* 44 (1979) 2203–2205;
 (b) J.J. Brunet, L. Mordenti, B. Loubinoux, P. Caubere, *Tetrahedron Lett.* 18 (1977) 1069–1072;
 (c) S. Masamune, G.S. Bates, P.E. Georghiou, *J. Am. Chem. Soc.* 96 (1974) 3686–3688;
 (d) J. Lipowitz, S.A. Bowman, *J. Org. Chem.* 38 (1973) 162–165;
 (e) P. Gallois, J.J. Brunet, P. Caubere, *J. Org. Chem.* 45 (1980) 1946–1950;
 (f) D.H. Gibson, Y.S. El-Omrani, *Organometallics* 4 (1985) 1473–1475;
 (g) E. Keinan, D. Perez, *J. Org. Chem.* 52 (1987) 2576–2580;
 (h) Y. Fort, R. Vanderesse, P. Caubere, *Tetrahedron Lett.* 27 (1986) 5487–5490;
 (i) K.E. Kim, S.B. Park, N.M. Yoon, *Synth. Commun.* 18 (1988) 89;
 (j) K.R. Russell, *e-EROS Encyclopedia of Reagents for Organic Synthesis*, John Wiley & Sons, Inc., 2001.
- [18] (a) M. Scommovigo, H. Alper, *Tetrahedron Lett.* 34 (1993) 59–62;
 (b) I.S. Cho, H. Alper, *J. Org. Chem.* 59 (1994) 4027–4028;
 (c) H. Jiang, D. Song, *Organometallics* 27 (2008) 3587–3592;
 (d) A.M. Caporusso, G. Giacomelli, L. Lardicci, *J. Org. Chem.* 47 (1982) 4640;
 (e) Z. Yang, M. Ebihara, T. Kawamura, *J. Mol. Catal. A: Chem.* 158 (2000) 509–514;
 (f) C.A. Mebi, B.J. Frost, *Organometallics* 24 (2005) 2339–2346;
 (g) H.M. Ali, A.A. Naiini, C.H. Brubaker Jr., *J. Mol. Catal.* 77 (1992) 125–134;
 (h) H.M. Ali, A.A. Naiini, C.H. Brubaker Jr., *Tetrahedron Lett.* 32 (1991) 5489–5492;
 (i) R. van Asselt, C.J. Elsevier, *J. Mol. Catal.* 65 (1991) L13–L19;
 (j) Y. Himeda, N. Onozawa-Komatsuzaki, S. Miyazawa, H. Sugihara, T. Hirose, K. Kasuga, *Chem. Eur. J.* 14 (2008) 11076–11081;
 (k) H. Jiang, E. Stepowska, D. Song, *Eur. J. Inorg. Chem.* (2009) 2083–2089;
 (l) J.H. van Tonder, C. Marais, D.J. Cole-Hamilton, B.C.B. Bezuidenhout, *Synthesis* 3 (2010) 421–424;
 (m) M. Mirza-Aghayan, R. Boukherroub, M. Bolourtchian, M. Rahimifard, *J. Organomet. Chem.* 692 (2007) 5113–5116.
- [19] (a) T. Kimura, T. Takahashi, M. Nishiura, K. Yamamura, *Org. Lett.* 8 (2006) 3137–3139;
 (b) P. Goswami, S. Ali, Md.M. Khan, B. Das, *Lett. Org. Chem.* 5 (2008) 659–664.
- [20] (a) J.A. Trejo, J. Tate, D. Martenak, F. Huby, S.M. Baxter, A.K. Schultz, R.J. Olsen, *Top. Catal.* 53 (2010) 1156–1162;
 (b) E.O.C. Greiner, C. Funada, *The Chemical Economics Handbook (CEH)*, SRI Consulting Report Number 675.6000, 2008.
- [21] (a) J.I. Di Cosimo, G. Torres, C.R. Apesteguía, *J. Catal.* 208 (2002) 114–123;
 (b) K.H. Lin, A.N. Ko, *Appl. Catal. A: Gen.* 147 (1996) L259–L265;
 (c) P.Y. Chen, S.J. Chu, K.C. Wu, W.C. Lin, U.S. Pat. 5684207, 1997;
 (d) L.V. Mattos, F.B. Noronha, J.L.F. Monteiro, *J. Catal.* 209 (2002) 166–176;
 (e) R.H. Crabtree, P.T. Anastas, *Green Catalysis: Heterogeneous Catalysis*, Wiley-VCH Verlag, 2009.
- [22] (a) L.P. Bevey (Ed.), *Progress in Catalysis Research*, Nova Science Publisher, Inc., New York, 2005, p. 178;
 (b) N. Cheikhi, M. Kacimi, M. Rouimi, M. Ziyad, L.F. Liotta, G. Pantaleo, G. Deganello, *J. Catal.* 232 (2005) 257–267;
 (c) M. Mediavilla, L. Melo, Y. Díaz, A. Albornoz, A. Llanos, J.L. Brito, *Micropor. Mesopor. Mater.* 116 (2008) 627–632.
- [23] (a) F. Maclean, C.C. Hobbs, US Pat. 2825743, 1955.;
 (b) J. Kasumi, M. Kuniyoshi, *Jpn. Pat.* 7215809, 1972;
 (c) Y. Qi, Z. Wang, R. Wang, *Appl. Catal.* 53 (1989) 63–70;
 (d) S. Nishimura, *Handbook of Heterogeneous Catalytic Hydrogenation for Organic Synthesis*, John Wiley & Sons, Inc., 2001, p. 226.
- [24] K.-H. Bergk, D. Woldt, Unpublished. See D. Woldt (1988) PhD Thesis, University of Halle-Wittenberg, Germany.
- [25] G. Lagaly, H. Tributh, *Ber. Dt. Tonmineralgruppe* (1991) 86.
- [26] T. Arthur, T.A. Stephenson, *J. Organomet. Chem.* 208 (1981) 369–387.
- [27] R.E. Grim, *Clay Mineralogy 4. Structure of Clay Minerals, Smectite Minerals*, McGraw-Hill, USA, 1968.
- [28] G. Meister, G. Süß-Fink, Unpublished. See G. Meister (1994) PhD Thesis, University of Neuchâtel, Switzerland.
- [29] M. Stebler-Röthlisberger, W. Hummel, P.-A. Pittet, H.-B. Bürgi, A. Ludi, A.E. Merbach, *Inorg. Chem.* 27 (1988) 1358–1363.
- [30] M.D. Abramoff, P.J. Magelhaes, S.J. Ram, *Biophotonics Int.* 11 (2004) 36–42.
- [31] (a) F. Delbecq, P. Sautet, *J. Catal.* 152 (1995) 217–236;
 (b) P. Sautet, J.F. Paul, *Catal. Lett.* 9 (1991) 245–260.